

Accepted Manuscript

Towards a prototype module for piezoelectric energy harvesting from raindrop impacts

Mohammad Adnan Ilyas, Jonathan Swingler

PII: S0360-5442(17)30245-1
DOI: 10.1016/j.energy.2017.02.071
Reference: EGY 10364
To appear in: *Energy*
Received Date: 25 September 2016
Revised Date: 09 January 2017
Accepted Date: 13 February 2017

Please cite this article as: Mohammad Adnan Ilyas, Jonathan Swingler, Towards a prototype module for piezoelectric energy harvesting from raindrop impacts, *Energy* (2017), doi: 10.1016/j.energy.2017.02.071

This is a PDF file of an unedited manuscript that has been accepted for publication. As a service to our customers we are providing this early version of the manuscript. The manuscript will undergo copyediting, typesetting, and review of the resulting proof before it is published in its final form. Please note that during the production process errors may be discovered which could affect the content, and all legal disclaimers that apply to the journal pertain.



Highlights:

- A technique is found to identify the efficiency of the impact mechanism
- A technique is also found for the mechano-electric conversion mechanism
- Values for the impact and conversion mechanism efficiencies are ascertained.
- The optimum arrangement for a single device is determined

Towards a prototype module for piezoelectric energy harvesting from raindrop impacts

Mohammad Adnan Ilyas¹ and Jonathan Swingler²

School of Engineering and Physical Sciences, Heriot-Watt University, United Kingdom, EH14 4AS

¹Email: a.ilyas@hw.ac.uk

²Email: j.swingler@hw.ac.uk

Abstract

It has been shown that scavenging energy from raindrop impacts has the potential as a power source for electronic devices and act as an alternative method of generating electrical power. In this paper an energy harvesting module is developed consisting of multiple piezoelectric devices which use impacts of raindrops to generate electrical power. The effect on efficiency of the module with non-rectified or rectified outputs of each device connected in parallel is investigated. Additionally, the voltage, power and energy were found for different surface angles, surface conditions and impact regions for single devices with a view to maximise module efficiency.

The main findings of this work are that: a) a technique is found to identify the efficiency of the impact mechanism as the droplet interacts with the device and the efficiency of the mechano-electric conversion mechanism due to internal losses in the device; b) values for the impact mechanism efficiency and the conversion mechanism efficiency are ascertained; and c) the optimum arrangement for a single device is determined.

Key words: Piezoelectric; Raindrop; Efficiency

32 **1. Introduction**

33

34 The energy crisis and environmental pollution have been some of the main challenges for
35 sustainable energy developmental [1]. Over the last decade there has been much research
36 focusing on mechanical vibrations [2], solar [3], wind [4], biomass [5], hybrid systems in a
37 combination of photovoltaic with thermoelectric generation [6], and electric vehicles with
38 photovoltaic generation [7] are some examples of renewable energy sources of all scales.
39 Energy harvesting offers an alternative approach, scavenging energy from the environment and
40 particularly useful for low power-consuming devices. Moreover, the potential of raindrop
41 impact energy harvesting has not been fully explored and this paper aims to propose a
42 piezoelectric energy harvester module and presents an investigation of its efficiency.

43

44 A previous study [8] focused on the voltage output caused by various velocities of water droplet
45 impacts on the harvester and showed that the oscillating voltage output has two distinct stages:
46 a growth followed by decay stage. The work presented in this new paper further builds on the
47 previous study. The effect of raindrop impacting the device at different regions, device angle
48 and surface condition are investigated. This study particularly investigates the power output
49 and efficiency of the single device and a multi-device module. The study shows that developing
50 a module of interconnected devices is not a trivial matter when trying to ensure the available
51 energy in the source is efficiently harvested. There are several points in the harvesting process
52 where energy is lost and this is discussed in detail in the paper.

53

54 **2. A Quick Review**

55

56 A quick review of the important aspects of piezoelectric raindrop energy harvesters is presented
57 focusing on devices developed and droplet surface interactions.

58

59 Piezoelectric materials have been used as a means of transforming externally available
60 vibrations into electrical energy that can be used to power devices and potentially store that
61 energy. With the recent surge of micro scale devices, piezoelectric power generation can
62 provide a convenient alternative to traditional power sources. However, the energy produced
63 by these materials in many cases has been reported to be very small and unable to directly
64 power a substantial electrical device. Therefore, much of the research into energy harvesting
65 has focused on methods of accumulating the energy until a sufficient amount is stored, allowing
66 the intended electronics to be powered for short periods.

67

68 The topic of energy harvesting using piezoelectric materials has attracted great interest in recent
69 years. The most common types of piezoelectric material being used are polyvinylidene fluoride
70 (PVDF) and lead zirconate titanate (PZT). The piezoelectric material consequently generates a
71 charge, which is collected by two electrode plates. The voltage created across the plates can be
72 defined as:

73

$$V = Q/C_{piezo}$$

74

75 Equation (1)

76 where Q is the charge generated and C_{piezo} is the capacitance of the material. The capacitance
77 can be expressed as:

78

$$C_{piezo} = \epsilon_0 \epsilon_r A/d$$

79

80 Equation (2)

81 where ϵ_0 is the electrical permittivity in vacuum, ϵ_r is the relative permittivity between the
82 electrode plates, A is the electrode area and d is the separation of electrode plates.

83

84 2.1 Raindrop Energy Harvesting

85

86 Raindrop energy harvesting techniques using piezoelectric materials simply convert the impact
87 energy and subsequent mechanical vibration of the device into an electricity supply. Most
88 previous studies on piezoelectric energy harvesting have concentrated on machine, human, and
89 other environmental sources of vibration. To date, a very limited number of studies have been
90 conducted on energy harvesting from raindrop impacts.

91

92 One of the most recent studies conducted by Nayan et al [9] showcased the need of developing
93 a rain harvester due to the favourable rainy condition in particular countries. The research
94 focused on series and parallel connected devices and proposed a design for the piezoelectric
95 plate. The output of the piezoelectric device was found to be dependent on the impact pressure
96 on the piezoelectric body. The voltage output was measured for different droplet heights and
97 simulations were carried out for different design approaches.

98

99 An in-depth study conducted by the current authors, Ilyas et al, [8] showcased detailed voltage
100 and power output from a piezoelectric device. This study was performed under laboratory
101 condition using different velocity of raindrop impacts and different electrical resistive load
102 conditions. The results showed two distinct stages to the oscillating voltage output consisting
103 of a relatively short duration growth stage followed by a longer decay stage. The study showed
104 the growth stage contributed a significant amount of the overall power output of the device
105 (total energy delivered of 90nJ and mean power of 2.5 μ W). Overall, the device efficiency was
106 found to be very low but suggestions were proposed for improvement. For example, it was
107 proposed efficiency could be significantly improved by modifying the droplet impact
108 mechanism with the harvester surface by exploring new surface materials to maximise inelastic
109 collision.

110

111 Another study by Guigon et al focused on PVDF materials with extensive work on theoretical
112 [10] and experimental models [11]. The main motivation of these studies was to review the
113 amount of energy that could be generated using these harvester types. The experimental set-up
114 consisted of a syringe pump as a source of water droplets and a piezoelectric system. The

115 syringe pump created identical droplet sizes for precision measurements and reproducibility.
116 Voltage was measured and energy calculated. The piezoelectric system consisted of two
117 transparent PVDF bands embedded in a Plexiglas structure. Various experiments were
118 conducted by changing the thickness of the PVDF beam which ranged from $9\mu\text{m}$ to $25\mu\text{m}$.
119 The study concluded that the thicker material ($25\mu\text{m}$) is more effective than the thinnest
120 material ($9\mu\text{m}$) at harvesting energy. Various impact situations were studied (different drop
121 heights and drop sizes) showing that the quantity of electrical energy that can be recovered
122 using these structure types is close to the proposed theoretical quantities, i.e. approximately 1
123 nJ of electrical energy and $1\mu\text{W}$ of instantaneous power using raindrops. The simulations
124 did not take into account the splash phenomena which may lead to reduction in energy transfer.

125
126 Another study [12] compared PVDF and PZT materials. The devices with these materials were
127 exposed under rain to determine the voltage levels generated by the impacts. The study
128 recommended the use of PVDF devices for raindrop energy harvesting because they showed
129 these generated higher power output.

130
131 Another study [13] focused on a device with a combination of cantilevers and diaphragm
132 structures forming the harvester. A comparison of empirical and simulation data was presented.
133 The prototype developed consisted of several layers namely: silicon, polyamide, Al
134 (aluminium), and a PVDF active layer. The focus in this work was on a meshed model of the
135 harvester. Results show a displacement pattern for the centre of the diaphragm with various
136 thicknesses of Al and PVDF. To achieve optimum results, thinner Al and PVDF are used, as
137 thickness is inversely proportional to maximum displacement. On the cantilever surface, as the
138 thickness of PVDF is increased the maximum displacement begins to decrease whereas the Al
139 is directly proportional to the maximum displacement. It is concluded that PVDF thickness of
140 150 nm and Al thickness of 35 nm results in a maximum displacement of 2800 nm . However,
141 at these thicknesses the maximum displacement on the centre of the diaphragm is relatively
142 small. These thicknesses are able to withstand the impact pressure of a large droplet of 13.718
143 MPa. The maximum displacement limit is found to be 2800 nm .

144
145 A theoretical review [14] focused on the proposal of the idea of a "Piezoelectric Shingle" as a
146 new energy harvesting system, based on meteorological precipitations as the rain. It presented
147 a preliminary analysis about the state of art of energy harvesting systems, based on
148 piezoelectric technology, showing potentiality, limits and other experiences in the field
149 of interest. It reviews the main features of rainy phenomena, interesting for an energy
150 harvesting system, reconsidering some theoretical/empirical models. Models are addressed
151 to define the limit velocity of raindrops and a distribution law between dimension of
152 raindrops and the nature of rainfall. After considerations about the annual quantity of water,
153 fallen in a region, the authors propose the ideation of some key patterns for a piezoelectric
154 energy harvesting system from rainy precipitations.

155
156 Maximum power output using a water vortex [15] on a macro fibre composite piezoelectric
157 energy harvester was found to be around $1.32\mu\text{W}$ with a water velocity of 0.5 m/s at the

158 cylindrical diameter of 30mm. By using an upright vortex-induced piezoelectric energy
159 harvester [16] the power output was found to be 84.49 μW using a velocity of 0.35 m/s.
160

ACCEPTED MANUSCRIPT

2.2 Surface Interaction

The fluid mechanics of droplet impact with a surface is of importance in a variety of different fields. The fluid flow associated with impinging drops is nontrivial and not fully described in detail in the scientific literature. A raindrop impact on a liquid surface can splash or bounce as well as merge with any surface liquid whereas a raindrop impact on a solid surface will either splash or spread out on the surface. The phenomenon is discussed in more detail in an earlier publication [8].

For the purpose of this study a comparison is conducted for droplet impact on liquid and solid surfaces as both would be seen in the real application. A detailed study conducted by Rein [17] reviewed different scenarios of droplet impact. The liquid is described by its thermodynamic state, and by its surface tension, viscosity and compressibility. Most theoretical and numerical calculations in the publication are based on the assumption that the drops are spherical. Due to aerodynamic forces the shape of drops moving through a fluid will always be rendered slightly ellipsoidal. Another study looked at mixing water and gelatine to form well defined non-spherical shape droplets [18] and draw a comparison of the output.

Another feature to take into consideration is that the harvester surface can generally be either smooth or rough. It is reported [19] that splashing is reduced when highly polished surface are used. At small surface roughness the splashing threshold depends strongly on the roughness, whereas the threshold is little influenced by the surface roughness when it is large. In many problems the elastic response of the surface is insignificant. However, the elasticity of the surface can no longer be neglected when high speed drops collide with a surface.

During the initial stage of impact the drop is merely deformed and compressed at its base. Hence, surface tension forces and the viscosity of the liquid do not enter the scenario at this stage. The important parameters are density and compressibility of the liquid, and the impact velocity and diameter of the drop. In the contact zone between the drop and the surface pressure is not uniform. It is highest at the contact edge where it exceeds the Waterhammer Pressure, and is lowest at the centre. This is due to the spherical geometry of the drop [19].

Splashing is a phenomenon often observed during liquid droplet impact onto a solid surface. The threshold of splashing is known to be related to droplet size, impact velocity, and physical properties of the liquid, but the mechanisms that initiate splashing are not understood completely. In accordance with the Kelvin-Helmholtz (K-H) instability analysis, recent studies [20] have shown that ambient gas density has a significant effect on the threshold and trajectory of splashing. Research has focused on the effects of droplet velocity, impact angle, and ambient gas pressure (or density) on the threshold of splashing and the motion of the ambient gas surrounding the droplet was examined. Experimental observations of splashing were carried out with a droplet of 1.7 mm in diameter, while varying droplet velocity, impact angle, and ambient pressure. An empirical correlation was derived using our and other published data to determine the threshold of splashing based on the aforementioned parameters. Also, a numerical simulation using the volume of fluid method was carried out to calculate the gas

205 velocities surrounding the droplet during impact. The results of this model gave supportive
206 evidence that K-H instability is a suitable instability theory that helps explain the splash
207 phenomenon with consideration of the gas motion surrounding the droplet

208

209 The ultimate aim is to present a combined energy harvesting technique that could use several
210 sources to power low-consumption devices and self-powered systems. The study on
211 triboelectric nanogenerator [21] has opened up new areas to be explored; for converting
212 mechanical energy to electrical energy with conversion efficiency at 60%. A review on
213 stretchable nanogenerators [22] showcased the potential of powering low-power devices with
214 high conversion efficiency. It has been reported that the energy conversion efficiency is
215 between 50% and 85%.

216

217 3. Methodology

218 3.1 Experimental Set-up

219

220 Water droplets are made to fall onto the piezoelectric device under laboratory conditions. The
 221 velocity of the droplets and thus the kinetic energy associated with them are calculated from
 222 the height of the droplet fall. Table 1 represents the velocity attained for the water droplet at
 223 various heights as previously published [8].

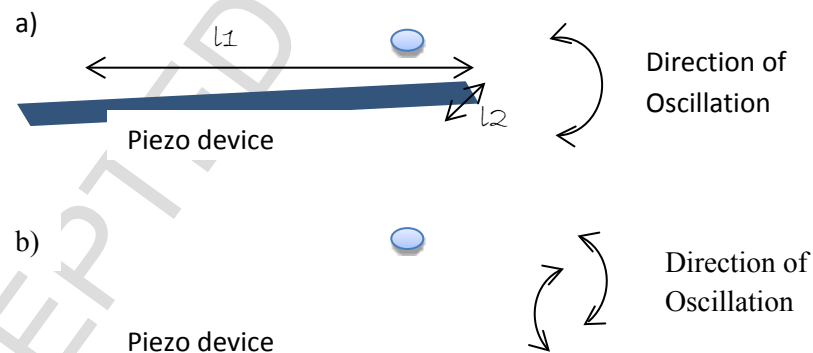
224

Velocity (m/s)	Kinetic Energy (μJ)
1.28	27.43
1.62	43.95
1.89	59.81
2.13	75.97

225 **Table 1:** Table: Kinetic energy of water droplets [8]

226

227 The device is mechanically fixed at one end so that it is free to move at the other end so that it
 228 can oscillate in a bending motion in the vertical direction. Figure 1a represents a device beam
 229 fixed at the left-hand side which has a water droplet impacting on the surface allowing it to
 230 oscillate along the length of the device (a pitching motion). This causes compressions and
 231 extensions in the piezoelectric material resulting in the charge displacements and energy
 232 conversion mechanism. Additionally, there are further possible vibrational modes, for example,
 233 in the wide of the device as in Figure 1b (a rolling motion).



234

235

236

Figure 1: Impact of Water droplets

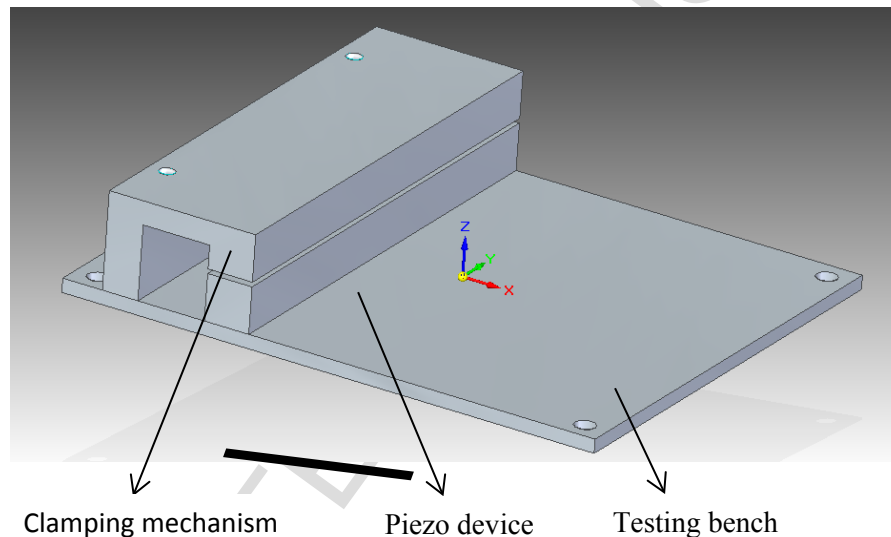
237 A commercially available piezoelectric device by Pro-Wave (FS-2513P) is used in this study.
 238 The piezoelectric film is coated with non-conductive material and has silver (Ag) electrodes
 239 on top and bottom of piezoelectric film.

240

241 The device is fitted in a test facility made of Perspex and is anchored on a stainless steel plate
 242 with rotary protractor to measure the angle of incline of the device (see Figure 2). The device
 243 is clamped into position on the test bench. The voltage output of the device is measured using
 244 a Digital Oscilloscope (Tektronix – TDS3032B) with differential probes (Testec – TTS19001).
 245 The probe was set at an attenuation of 1/10. Each test was repeated several times (usually 4
 246 data points collected) to show reproducibility of the data.

247

248 The test facility allows consistency of clamping the device into position and flexibility of
 249 connecting various devices either in series or parallel to form a module. The device is simply
 250 slotted into the clamping mechanism which is made of rubber to provide firm support to the
 251 device.



252

253

Figure 2: Test facility

254

255 The table below specifies the experimental parameters:

Dimension of device	25 x 13 x 3 mm
Capacitance of device	1.5 nF \pm 30%
Load connected	1M Ω
Operational temperature	-20 to +60 °C
Range of Angle	0 to 45 °

256

257

258

259 Three impact regions are identified on the piezoelectric device surface as illustrated in Figure
 260 3 for targeting of the droplet. The device is clamped towards the left-hand side as illustrated
 261 allowing the right-hand side of the device to move up/down freely. Voltages with time
 262 measurements are taken by using a Digital Oscilloscope.

263
264
265
266
267
268
269
270
271
272
273
274
275
276
277
278
279
280

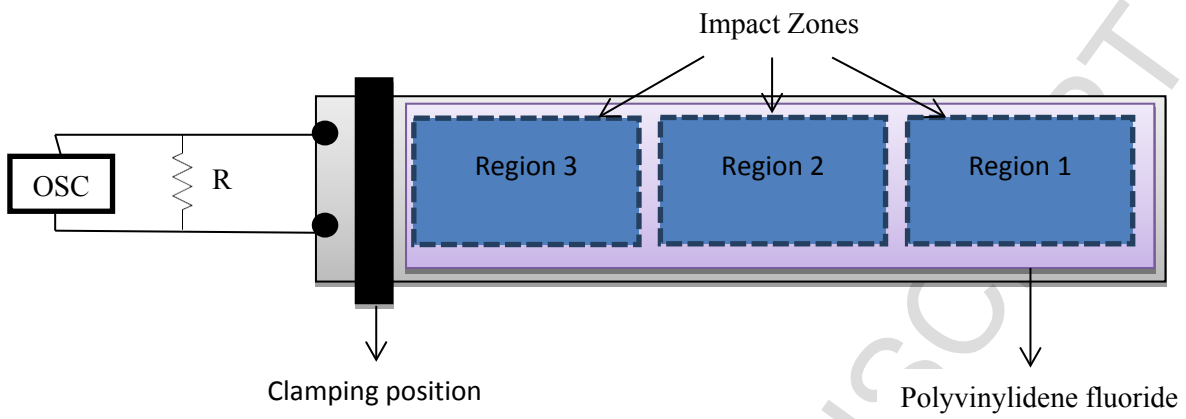


Figure 3: Impact Zones

281 3.2 Single and Multiple Device Module

282

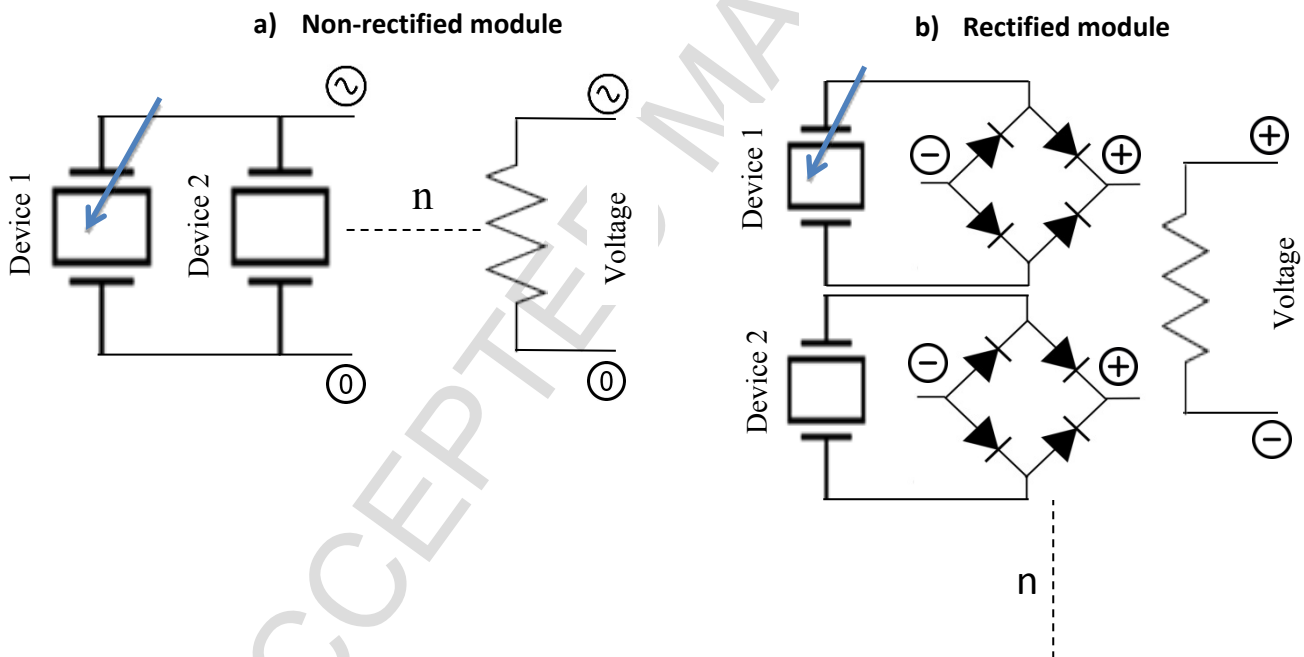
283 For the single device tests, a single device is connected to the $1\text{ M}\Omega$ resistive load and the
 284 voltage across the load captured on a digital oscilloscope. Figure 4a shows the general
 285 configuration. Tests are repeated a least 4 times for any one configuration.

286

287 The first series of tests with multiple devices is conducted with a number of devices connected
 288 in parallel to make a module which is connected in turn to the $1\text{ M}\Omega$ resistive loads. The general
 289 configuration is illustrated in Figure 4a. The voltage output across the load is measured with
 290 time. During these tests on multiple devices, only one device is activated by the impact of water
 291 droplets as indicated by the arrow in Figure 4a. Tests are repeated at least 4 times for any one
 292 configuration.

293

294 The second series of tests with multiple devices is conducted with each device having its own
 295 rectification component and then these are connected in parallel to make up a module. These
 296 are then connected to the $1\text{ M}\Omega$ resistive loads. The general configuration is shown in Figure
 297 4b. During these tests on rectified multiple devices, only one device is activated by the impact
 298 of water droplets as indicated by the arrow in Figure 4b. Tests are repeated at least 4 times for
 299 any one configuration.



300

301

302 **Figure 4:** Circuit diagram (a) non-rectified module, (b) rectified module

303

304

305

306

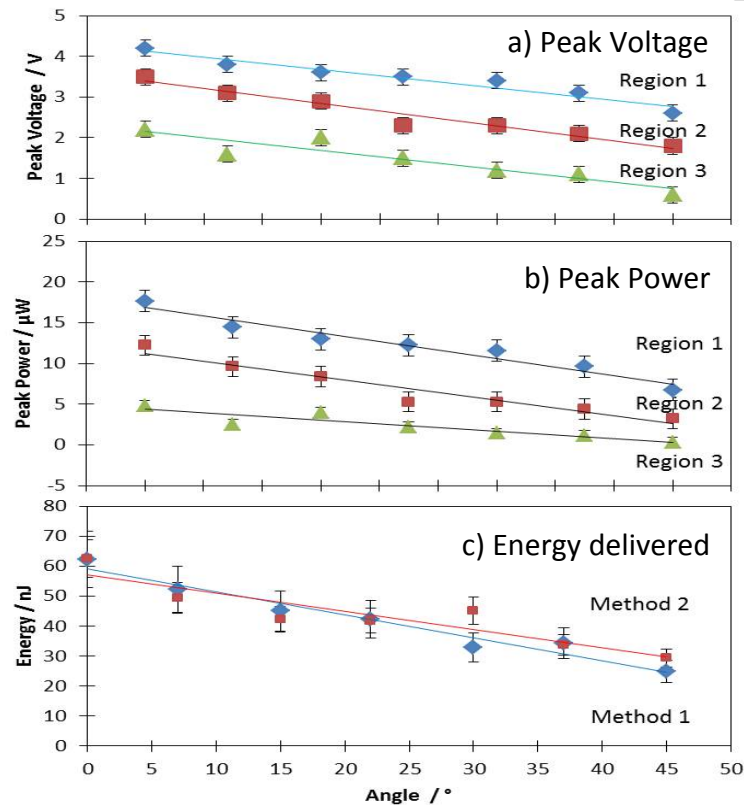
307

308 4. Results

309 4.1 Single Device Study

310 4.1.1 Voltage Measurements

311 Peak voltage over the three regions was measured over surface angle at which the device is
 312 declined. As discussed earlier, the impact mechanism plays an important role in the overall
 313 output of the device. The results in Figure 5a demonstrate that Region 1 gives out maximum
 314 voltage when the device anchored at horizontal position (surface angle set as 0°), therefore for
 315 all other calculations results obtained from Region 1 will be used.



316

317 **Figure 5:** Parameters of single device (a) Peak voltage, (b) Power output from harvester, (c)

318

Energy output using method 1 and 2

319

320 The results are consistent with what was expected with different regions on the device.
 321 Experiments were conducted against different angles to deduce the best region and angle to
 322 drive maximum output. As the angle of the device is increased from 0° to 45° it was observed
 323 that the peak voltage decreases. This can be due to the impact position of the droplet. When
 324 the device is at 0° the droplet normally splashes on the device and most of it is retained on the
 325 surface of the device hence giving a higher output. When the droplet impacts the device at an
 326 angle most of it disperses and bounces off the device hence a lower output is observed. The
 327 peak power attained was in the region of 4 to 18 μW which is in line with the set of data
 328 obtained in the first publication.

329

330 Peak voltages were also measured additionally to study various surface conditions on the
 331 device. The results shown in Table 3 are for a resistive load of $1\text{M}\Omega$, 0° at Region 1. The
 332 surface conditions are altered by using cellulose based tape and vinyl based tape. The results
 333 do not show any significant change in the peak output voltage of the device.

Surface	Peak Voltage (V) ($\pm 0.2\text{V}$)
Dry surface on sensor	2.9
Wet surface on sensor	3.0
Transparent Tape (Cellulose based)	2.9
Transparent Tape (Cellulose based) with holes	2.8
Insulation Tape (Vinyl based)	3.0
Insulation Tape (Vinyl based) with holes	2.9

345
 346 **Table 3:** Peak voltage at various surface conditions

348 A series of results were captured for the ramp-up (initial impact) of water droplet to impacting
 349 on a dry and wet device. For consistency and repeatability the resistive load was $1\text{M}\Omega$, with 0°
 350 angle and impacting at Region 1.

351 For the dry condition, the device was wiped clean before every reading was taken. Any water
 352 droplets that may have been deposited on the surface of the device were wiped dry before each
 353 set of results were saved. This shows an ‘edgy’ initial impact with the surface of the device.
 354 The wet device replicates real rain conditions where the water droplets may already be
 355 deposited on the surface of the device. The results show a smoothing of initial impact as the
 356 water droplet impacts the surface of the device. The two different waveforms are shown in
 357 Figure 6.

358 a) Dry device

359
 360
 361
 362
 363
 364
 365 b) Wet device

366
 367
 368
 369
 370
 371
 372
 373

Figure 6: Device output in different conditions (a) Dry device, (b) Wet device

374 As explained earlier there may be multiple modes of oscillation; vertical oscillations and width-
 375 ways oscillations. The dry device in Figure 6a shows the initial impact as a ‘high-frequency
 376 wobble’. When the water droplet interacts with the surface of the device it can possibly be
 377 oscillating the device sideways thus giving us an edgy curve. Figure 6b shows a ‘low-frequency
 378 wobble’ as the curve is smoothed out indicating that the device has only oscillated in vertical
 379 direction. The difference between the peak voltage of wet and dry device is negligible.
 380 However, we have determined that the surface interaction and the way the device oscillates is
 381 of importance and needs further studies conducted to understand the behaviour of these
 382 oscillations.

383

384 The dominant fact is whether the device is dry or wet the peak voltage remains the same. The
 385 difference in the waveform in Figure 6 can be further explained by assuming the material is
 386 homogenous in every direction therefore the ‘k’ is defined as a constant and the two equations
 387 can be brought together as in Equation 3.

388

$$f_1 = \frac{k}{l_1}, f_2 = \frac{k}{l_2}$$

389

$$f_1 l_1 = f_2 l_2$$

390

Equation Set (3)

391

392

393 4.1.2 Peak Power & Energy Delivered

394

395 The instantaneous peak power (P) has been determined using Equation 4 for the data collected.
 396 The resistive load (R_{load}) in this experiment was set as $1M\Omega$ ($\pm 5\%$) and peak instantaneous
 397 power was calculated as shown in Figure 5b.

398

$$399 \text{ Power} = V^2 / R_{load}$$

400 Equation (4)

401

402 The energy delivered to the load is calculated from the voltage data collected by two methods:

403 Method 1:

404 As detailed in our previous publication the impact of water droplet on the piezoelectric device
 405 was broken into two stages; log growth and exponential decay. The energy graph of the
 406 harvester is plotted in Figure 5c. The energy output of the impact was found by these steps:

- 407 - Instantaneous power was calculated for each data point using equation 4 and the
- 408 average found.
- 409 - The duration of log growth (t_1) and exponential decay (t_2) was determined.
- 410 - Energy was calculated using equation (5).

411

412

$$413 E = (\langle P_g \rangle \times t_1) + (\langle P_d \rangle \times t_2)$$

414

Equation (5)

415 Method 2:

416 The energy output of the impact was found by these steps:

- 417 - Instantaneous power was calculated for each data point using equation 4.
- 418 - The time step for each data point, t_s , is calculated to be 0.00004 seconds.
- 419 - Energy was calculated using equation (6).

420

421
$$E = \sum_0^n (P_g \times t_s) + \sum_x^y (P_d \times t_s)$$

422

Equation (6)

423

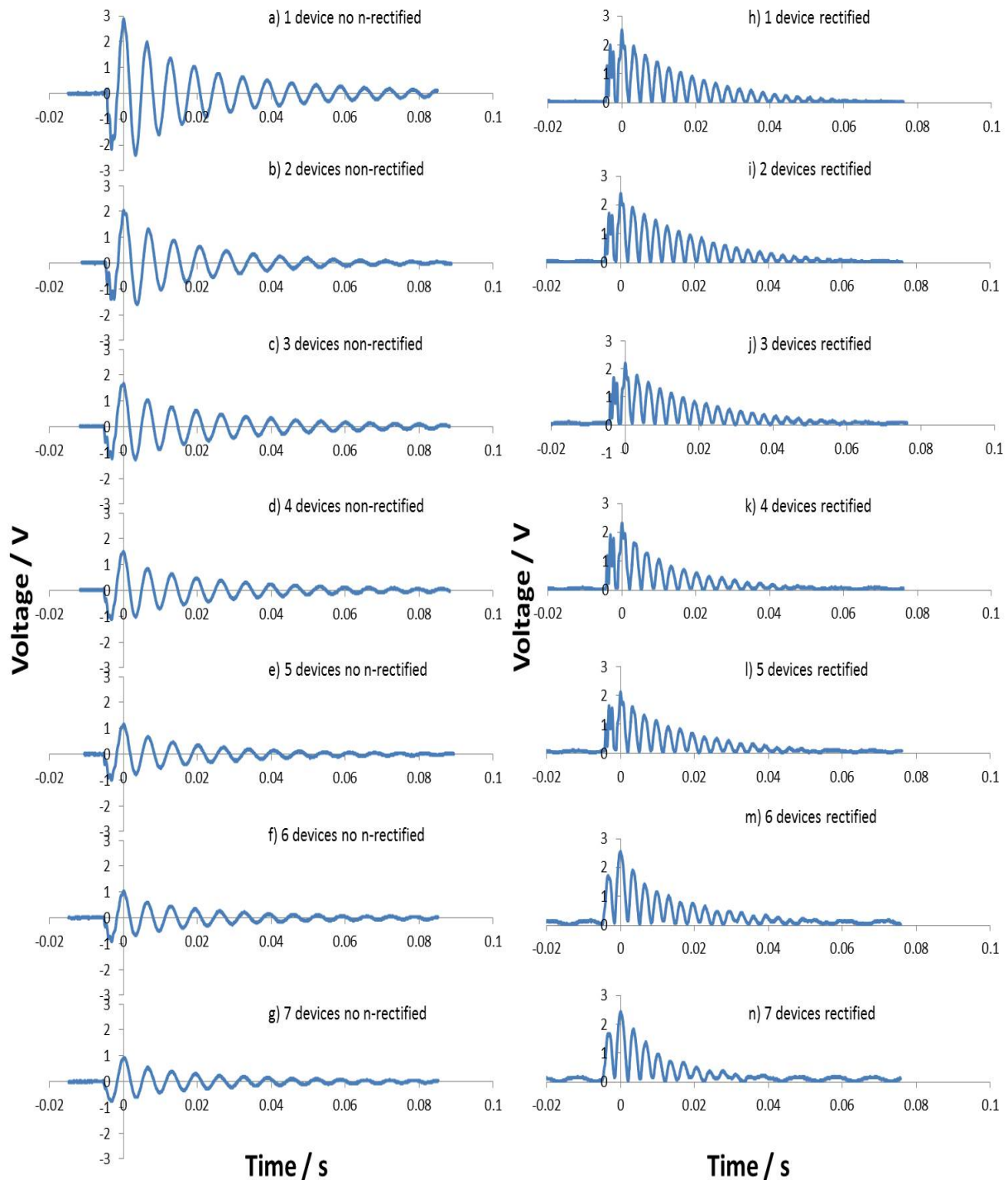
424

425 4.2 Multiple Device Module Study

426 4.2.1 Voltage Measurements

427

428 Figure 7 shows the voltage waveforms obtained for up to 7 devices connected in parallel. There
 429 is a decline in voltage as more devices are connected in parallel. The voltage ranges from 0.9V
 430 to 3.1V. The experiment was repeated several times to ensure consistent results and rule out
 431 any issues in data collection.



432

433

Figure 7: Voltage output with multiple devices connected in parallel

4.2.2 Peak Power & Energy Delivered

435

436 The peak power of module is calculated for devices connected in parallel. Figure 8a shows
 437 the peak power of the non-rectified devices and rectified devices in the module. The rms
 438 voltage of the non-rectified devices is plotted in Figure 8b. This output voltage is a function
 439 of n devices and is empirically modelled by equation (7)

440

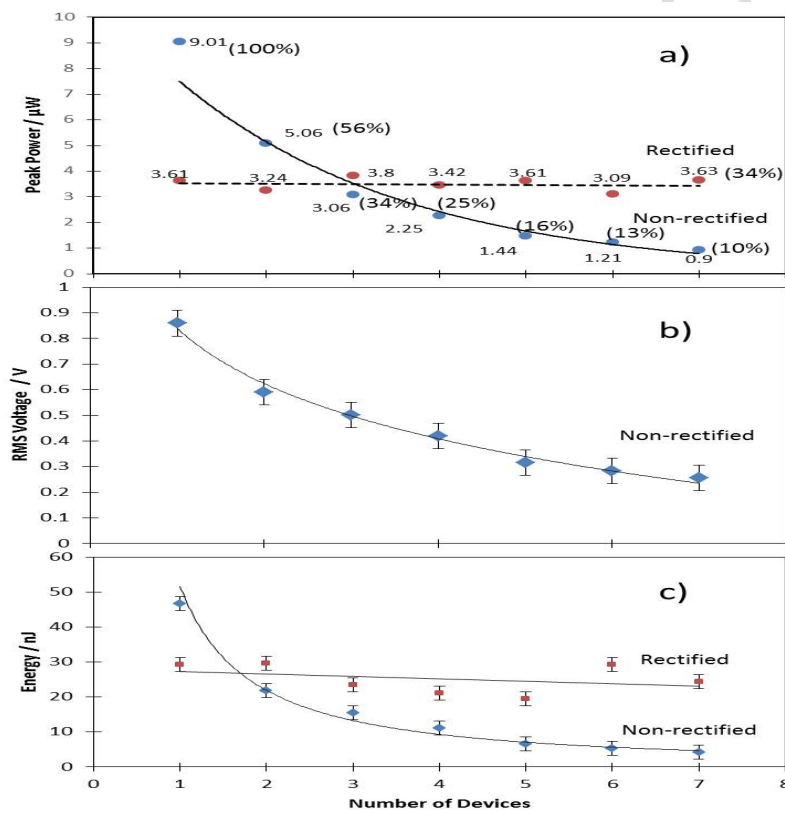
$$V_{em}(n) = 0.9117n^{-0.629}$$

441

Equation (7)

442 The Energy output of the module is shown in Figure 8c. The non-rectified module shows a
 443 significant decline in energy output as more devices are added in parallel in the module. There
 444 is a general decline in the energy output as more devices are added in parallel in the module.

445



446

447 **Figure 8:** Parameters of the module (a) Peak power, (b) rms voltage, (c) Energy delivered

448

449

5. Analysis & Discussion

450
451
452
453
454
455
456
457
458
459
460
461
462
463
464
465
466
467
468
469
470

Limited research has been conducted in the field of raindrop energy harvesting. Results published earlier [8] demonstrated that piezoelectric materials can be effectively used to harness the energy of raindrop impacts. Detailed profile of the voltage output from the device was published which introduced the ‘log growth’ and ‘exponential decay’ stages. Even though the growth stage was the shortest stage but the impact process of the droplet had a significant contribution to the overall output of the device. The efficiency was found to be very low at the time with the old set-up and we have improved the set-up for this set of experiments to be able to closely examine the results and improve the efficiency.

It is found that the angle of device to the falling droplet have a significant effect on the output of the device. To maximise the power out, the device should be presented at 0° to the falling droplet and the droplet should impact the end of the device to generate the maximum bending mode of oscillation. The surface condition of the devices was also investigated and no significant effect was found. Of particular interest was whether an already water saturated surface of the device behaved differently to a dry surface; no significant effect was found.

5.1 Analysis of Multi-Device Data

The analysis of non-rectified devices is discussed in detail first before considered the effect of rectification. Figure 9a illustrates the equivalent circuit for one device which has an impact event of a droplet where the device is connected to n number of devices with no droplet impacts. The electrical power sources in Figure 9a indicates the power which has been captured from the droplet – that is, the power available after the impact mechanism. The droplet falls with a particular kinetic energy, E_{KE} , for example $75.97 \mu\text{J}$ as in Table 1, inelastically impacts the harvesting device. The droplet undergoes its impact mechanism with the water bouncing back and spreading across the surface taking a portion of the initial kinetic energy with it. Also, a proportion of this initial kinetic energy is captured, E_0 , by the device and mechanically sets the device in damped simple harmonic motion. The mechanical characteristic of this simple harmonic motion is modelled with the equivalent circuit of $L_m C_m R_m$ as in Figure 9a for Device 1. The L_m and C_m components model the behaviour of the transfer of kinetic and potential energy in the device as it vibrates. R_m models the mechanical losses. Also in Figure 9a for Devices 1 are equivalent components for electrical storage and losses. C_e is the capacitance of the device as it consists of two parallel plates across the piezoelectric and R_{e1} and R_{e2} are the electrical losses in the devices from, for example, current leakage across the piezoelectric.

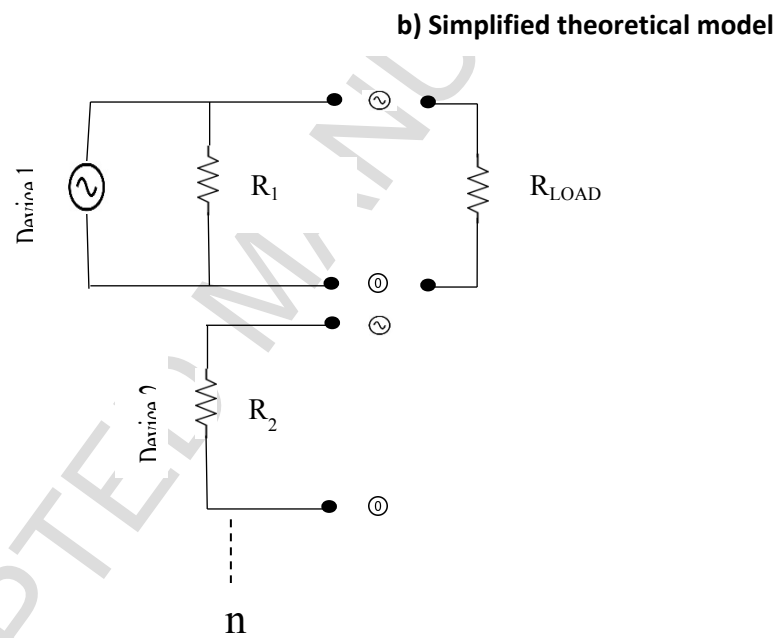
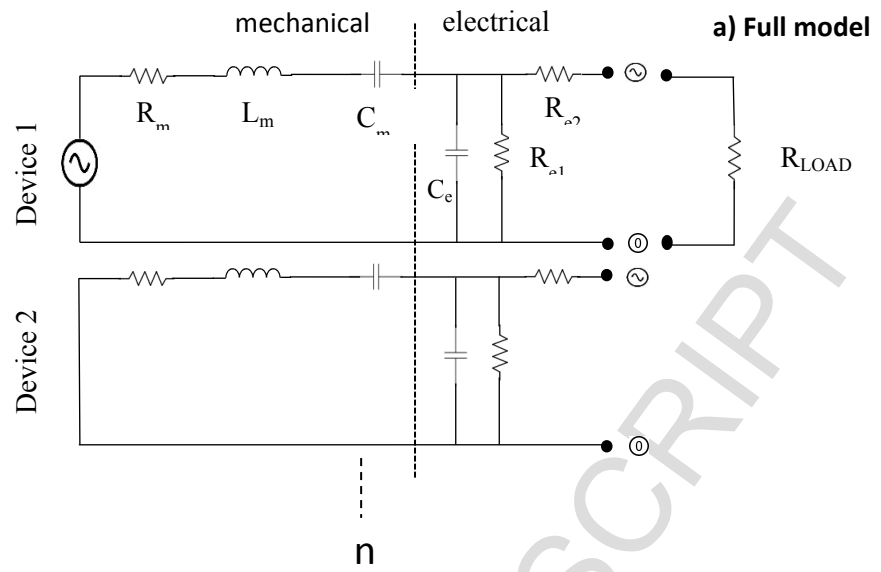
Device 2 and n devices connected to the active Device 1 which undergoes an impact event have no power sources in as at this impact event of Devices 1. However, as n devices are electrically connected, these connected devices will be excited by the electrical power produced by Device 1. This is modelled as in Figure 9a consisting of mechanical and electrical behavior modelled with the equivalent circuit.

Figure 9b is a simplified theoretical equivalent circuit of the n connected devices used to model the energy flow when Device 1 undergoes an impact event over the whole duration t_d of the event and damping of the vibration of the device, with duration of for example 0.06 s . The voltage drop across the source and load resistor R_{load} is given by Equation (8), the voltage of the simplified theoretical model (stm):

$$V_{stm}(n) = \left(\frac{E_0}{t_d}\right)^{0.5} \left(\frac{1}{R_{load}} + \frac{n}{R_0}\right)^{-0.5}$$

Equation (8)

It is assumed that the losses within each device are the same, such that $R_1 = R_2 = R_0$. R_0 is a component which lumps together all mechanical and electrical losses in a single device. It is also assumed that the energy captured from the droplet impacted is not a function of n devices connected. It is assumed that no energy is returned back to the remains of the droplet water from energy that was captured.



510

511

512

513

514

Figure 9: Equivalent Circuit Model of Multiple Connected Devices

515 5.2 Efficiency of the Impact Mechanism

516

517 Using the simplified theoretical model of Figure 9b and its Equation (8) with the experimental
 518 data empirically model in Equation (7), the energy captured from the impact mechanism E_0 can
 519 be found. This is the energy transferred from the droplet to the harvester as the droplet impacts
 520 the surface.

521

522 A simple procedure is presented which uses the decrease in the output voltage with the increase
 523 in n devices to extrapolate to give $V_{stm}(0)$, the excitation voltage of the device with no internal
 524 losses, to find E_0 :-

525 a) Plot experimental data (circle data points in Figure 10) and fit a trend line to acquired
 526 empirical model $V_{em}(n)$. The best fit is a power function which is valid between the
 527 limit of $\{7 \geq n \geq 1\}$ and thus $V_{em}(0)$ cannot be found.

528 b) Find the change in V_{em} with the change in the number of device n for each n , $\Delta V_{em}/\Delta n$,
 529 from the empirical model $V_{em}(n)$ data. These data points are plotted as triangle on
 530 Figure 10.

531 c) Plot a best fit line for $\Delta V_{em}/\Delta n$ data to give $dV_{em}(n)/dn$ and extrapolate back to $n=1$ The
 532 data point for $n=1$ is plotted as a square in Figure 10.

533 d) Therefore the change is V_{em} from $n = 0$ to $n = 1$ can be found and thus $V_{stm}(0)$ is
 534 estimated. This value is plotted as a diamond data point in Figure 10. $V_{stm}(n)$ can be
 535 plotted once R_0 is found (see section 5.3). This is plotted as a dotted line on Figure 10.

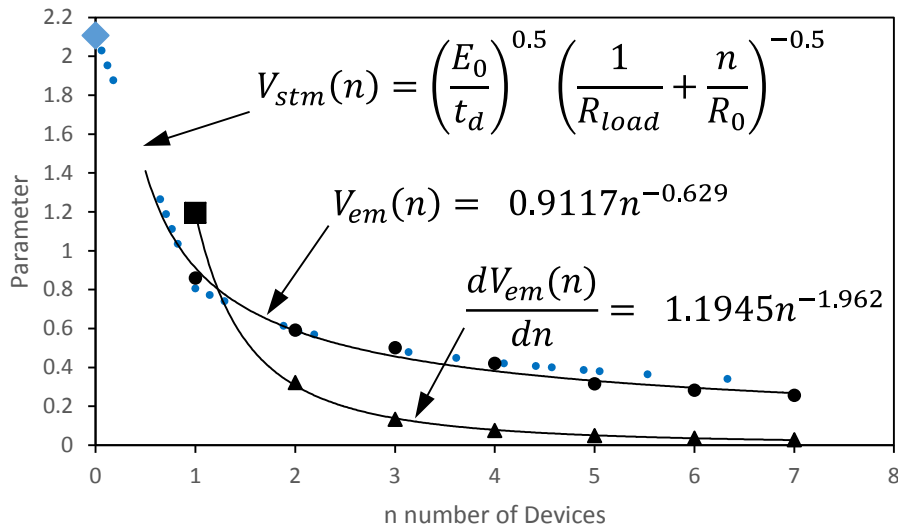


Figure 10: Finding the Excitation Voltage $V_{stm}(0)$

536 Using the data from the experiments for the velocity of droplet at 2.13 m/s, $V_{stm}(0)$ is found to
 537 be 2.106 ± 0.11 V. Given that the whole harvesting process duration is t_0 , estimated at 0.06 s,
 538 E_0 is found to be 266.2 ± 29 nJ. Table 1 gives values for the kinetic energy of drops and thus
 539 the efficiency of the impact mechanism can be estimated and is found to be 0.350 ± 0.054 %.

540

541 5.3 Efficiency of the Mechano-Electric Conversion Mechanism

542

543 Again, using the simplified theoretical model of Figure 9b and its Equation (8) with the
 544 experimental data empirically model in Equation (7), and also knowing the energy captured
 545 from the impact mechanism E_0 , the losses within a harvest R_0 can be found. This is realised by
 546 using a numerical method by inputting trial values of R_0 in Equation (8) to find best fit to the
 547 experimental data empirically model by Equation (7). This analysis is shown in Figure 11 with
 548 3 trial values of R_0 . Giving an estimate of $R_0 = 170 \pm 30 \text{ k}\Omega$.

549

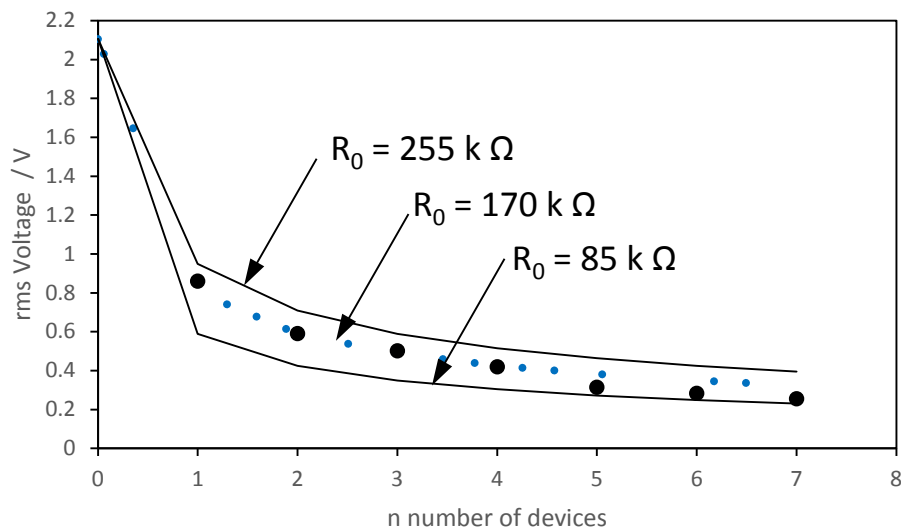


Figure 11: Finding the Internal Resistance (losses) R_0 of a Harvester

550 The energy delivered by a single device is found to be $51 \pm 12 \text{ nJ}$, see Figures 5c and 8c. This
 551 energy comes from the energy delivered by the impact mechanism which is $266.2 \pm 29 \text{ nJ}$
 552 giving an efficiency for the mechano-electric conversion mechanism as $0.334 \pm 0.073 \%$

553

554 5.4 Efficiency With and Without Rectification

555

556 The overall efficiency of a single device without rectification is found to be $0.671 \pm 0.158 \%$.
 557 By adding further devices in parallel in a harvesting module (without rectification) reduces the
 558 efficiency of the output during a single droplet impact. With 7 devices, the efficiency is reduced
 559 to 10% of the case with a single device. This is due to the additional devices being excited by
 560 the one device which has the droplet impact. A way to overcome this is to prevent the additional
 561 devices from being excited. One means is to use semiconductor diode rectification.

562

563 The rectified devices were connected in parallel to build a module of up to 7 devices. A
 564 disadvantage with using the silicon diode technology is that there is a voltage drop of the silicon

565 diode of around 0.7 V. The effect of this can be seen in the results. For the single device case,
566 there is a drop of power output from the non-rectified device to the rectified device. As Figure
567 8c illustrates the rectified case maintains a constant power out as a function of n device which
568 is around 34% of the single device non-rectified case. Using rectification ensures that the
569 efficiency to not full with increasing number of device n as in the non-rectified case.

570

571 **5.5 Application & Future Work**

572 Due to the limitation of active piezoelectric material used in this study, the output of such a
573 device is very low which therefore means it is likely be used in conjunction with other
574 technologies such as photovoltaic or thermoelectric generators. The findings in this study will
575 help develop a device that can be optimised as part of a combined energy harvesting device for
576 consumer electronics with low power input. The device can be further integrated in remote
577 locations where access to the grid is intermittent or non-existent.

578

579 For applications in low-power consumer devices, piezoelectric materials are required with the
580 properties of wide degree of freedom in shapes and stretchable characteristics. These properties
581 can then open various other applications beyond hand-held devices to wearable energy
582 generating sources. Future work will comprise of fabricating piezoelectric materials with high
583 piezoelectric property and sustainable material. In this study we have used commercially
584 available materials that are not specifically designed to harvest energy using impact of
585 raindrops. This study explored the effect of rectification which used silicon diodes with a
586 voltage drop of around 0.7V, future experiments will be conducted on diodes with a very low
587 voltage drop.

588

589 Another area to explore would be increasing the output of such a device by improving the
590 conversion efficiency. The next stages of this work will focus on improving the impact, electro-
591 mech and connection efficiencies. In addition, the devices will be trialled in real rainstorm
592 presenting an opportunity to investigate the behaviour of devices in such conditions.

593

594

595

596

597

598

599

600

601

602

603

604

6. Conclusion

This paper presents voltage output of piezoelectric device using the active material Polyvinylidene fluoride under the impact of water droplets. Piezoelectric device was connected to resistive load and voltage measurements were taken to calculate the output of the device.

The effect on efficiency of the module with non-rectified or rectified outputs of each device connected in parallel is investigated. Additionally, the voltage, power and energy were found for different surface angles, surface conditions and impact regions for single devices with a view to maximise module efficiency.

The main findings of this work are that: a) a technique is found to separate the efficiency of the impact mechanism as the droplet interacts with the device and the efficiency of the mechano-electric conversion mechanism due to internal losses in the device; b) values for the impact mechanism efficiency and the conversion mechanism efficiency; and c) the optimum arrangement for a single device.

The energy delivered from the impact mechanism E_0 is found to be 266.2 ± 29 nJ. Given 7,597nJ of kinetic energy in the falling droplet, the efficiency of the impact mechanism is estimated to be 0.350 ± 0.054 %. The energy delivered from the device is found to be 51 ± 12 nJ. Given 266.2 ± 29 nJ of energy from the impact mechanisms, the efficiency of the mechano-electric conversion mechanism is estimated to be 0.334 ± 0.073 %. The overall efficiency of a single device is found to be 0.671 ± 0.158 %. Adding further devices to make a multi-device module further reduces the efficiency as other devices are a source of power loss for any one device that is impacted by a droplet. Rectification on the output of each device does improve the performance for a multi-device module.

One of the main contributions this work makes is that there are three points in the harvesting process where energy can be lost. This work also shows how to separate impact efficiency from mech-elec conversion efficiency. It also shows that care needs to be taken in interconnecting devices. All these aspects have not been published before.

Acknowledgement

This work is partially funded by the Doctorial Training Account of the UK's research councils.

639 **References**

640

- [1] S. M. Lele, "Sustainable development: A critical review," *Word Development*, vol. 19, no. 6, pp. 607-621, 1991.
- [2] C. Grouthier, S. Michelin, R. Bourguet, Y. Modarres-Sadeghi and E. de Langre, "On the efficiency of energy harvesting using vortex-induced vibrations of cable," *Fluids and Structures*, vol. 49, pp. 427-440, 2014.
- [3] F. Martins, S. Abreu and E. Pereira, "Scenarios for solar thermal energy applications in Brazil," *Energy Policy*, vol. 48, pp. 640-649, 2012.
- [4] C. Ilkilic and I. Turkbay, "Determination and utilization of wind energy potential for Turkey," *Renewable and Sustainable Energy Reviews*, vol. 14, pp. 2202-2207, 2010.
- [5] R. Spinelli, N. Magagnotti, C. Nati, C. S. G. Cantini, G. Picchi and M. Biocca, "Integrating olive grove maintenance and energy biomass recovery with a single-pass pruning and harvesting machine," *Biomass and Bioenergy*, vol. 35, pp. 808-813, 2011.
- [6] J. Zhang, Y. Xuan and L. Yang, "Performance estimation of photovoltaic-thermoelectric hybrid systems," *Energy*, vol. 78, pp. 895-903, 2014.
- [7] F. Fattori, N. Anglani and G. Muliere, "Combining photovoltaic energy with electric vehicles, smart charging and vehicle-to-grid," *Solar Energy*, vol. 110, pp. 438-451, 2014.
- [8] M. A. Ilyas and J. Swingler, "Piezoelectric energy harvesting from raindrop impacts," *Energy*, vol. 90, no. 1, pp. 796-806, 2015.
- [9] N. M. Nayan, M. F. A Razak, A. Ali, S. K. Mazalan, A. N. N. Abdullah and N. H. Rahman, "Development of rain harvester using piezoelectric sensor," in *International Conference on Power, Energy and Communication Systems*, Perlis, 2015.
- [10] R. Guigon, J. Chailout, T. Taget and G. Despesse, "Harvesting raindrop energy: Theory," *Smart Material and Structures*, vol. 17, no. 1, 2008.
- [11] R. Guigon, J. Chailout, T. Taget and G. Despesse, "Harvesting raindrop energy: Experimental study," *Smart Material and Structures*, vol. 17, no. 1, 2008.
- [12] F. Viola, P. Romano, R. Miceli and G. Acciari, "Harvesting rainfall energy by means of piezoelectric transducers," in *Clean Electrical Power*, Alghero, 2013.
- [13] W. D. Z. Chin-Hong, "Simulation of piezoelectric raindrop energy harvester," in *TENCON*, Sydney, 2013.
- [14] R. D. LEO, V. Massimo, F. Gianluca and L. Lecce, "Preliminary theoretical study about a "Piezoelectric Shingle" for a piezoelectric energy harvesting system in presence of rain," *Mathematical and computational methods in Electrical Engineering*, pp. 9-17, 2013.

- [15] X. Shan, R. Song, B. Liu and T. Xie, "Novel energy harvesting: A macro fiber composite piezoelectric energy harvester in the water vortex," *Ceramic International*, vol. 41, pp. 7633-767, 2015.
- [16] R. Song, X. Shan, F. Lv and T. Xie, "A study of vortex-induced energy harvesting from water using PZT piezoelectric cantilever with cylindrical extension," *Ceramics International*, vol. 41, pp. 768-773, 2015.
- [17] M. Rein, "Phenomena of liquid drop impact on solid and liquid surfaces," *Fluid Dynamics Research*, vol. 12, no. 1, pp. 61-93, 1993.
- [18] J. Field, M. Lessr and P. Davies, "Theoretical and experimental studies of two dimensional liquid impact," in *Erosion by Solid and Liquid Impact*, Cambridge, 1979.
- [19] D. G. K. Aboud and A.-M. Kietzig, "Splashing Threshold of Oblique Droplet Impacts on Surfaces of Various Wettability," *Langmuir*, vol. 31, no. 36, pp. 10100-10111, 2015.
- [20] J. Liu, H. Vu, S. Yoon, R. Jepsen and G. Aguilar, "Splashing phenomena during liquid droplet impact," *Atomization and Sprays*, vol. 20, no. 4, pp. 297-310, 2010.
- [21] Z. L. Wang, "Triboelectric nanogenerators as new energy technology and self-powered sensors - Principles, problems and perspectives," *Faraday Discussions*, vol. 176, pp. 447-458, 2014.
- [22] K. Y. Lee, M. K. Gupta and S.-W. Kim, "Transparent flexible stretchable piezoelectric and triboelectric nanogenerators for powering portable electronics," *Nano Energy*, vol. 11, 2014.
- [23] S. Trolier-Mckinstry and P. Muralt, "Thin film piezoelectrics for MEMS," *Journal of Electroceramics*, vol. 12, pp. 7-17, 2004.
- [24] G. K. Ottaman, A. C. Bhatt, H. Hofmann and G. A. Lesieutre, "Adaptive piezoelectric energy harvesting circuit for wireless remote power supply," *IEEE Transaction on Power Electronics*, vol. 17, pp. 669-676, 2002.
- [25] E. Zakar, "MEMS PIEZO PRESSURE SENSOR FOR MILITARY APPLICATIONS," U.S. Army Research Laboratory, Adelphi, 2004.
- [26] J. Rocha, L. Gonclaves, P. Rocha and S. Lanceros-Mendez, "Energy Harvesting from Piezoelectric Materials fully Integrated in Footwear," *IEEE Transactions on Industrial Electronics*, vol. 57, no. 3, pp. 813-819, 2010.
- [27] N. Ramer, T. Marrone and A. Stiso, "Structure and vibrational frequency determination for α -poly(vinylidene fluoride) using density-functional theory," *Polymer*, vol. 47, pp. 7160-7165, 2006.
- [28] B. Calhoun, D. Daly and N. Verma, "Design considerations for ultra-low energy wireless microsensor nodes," *IEEE TRANSACTIONS ON COMPUTERS*, vol. 54, no. 6, pp. 727-740, 2005.
- [29] A. Hajati and S. G. Kim, "Ultra-wide bandwidth piezoelectric energy harvesting," *Applied Physics Letters*, vol. 99, 2011.

- [30] R. Guigon, J. Chailout, T. Jager and G. Despesse, "Harvesting raindrop energy: theory," *Smart Materials and Structures*, vol. 17, 2008.
- [31] R. Guigon, J. Chailout, T. Jager and G. Despesse, "Harvesting raindrop energy: experimental study," *Smart Materials and Structures*, vol. 17, 2008.
- [32] R. Martin, "Phenomena of liquid drop impact on solid and liquid surfaces," *Fluid Dynamics Research*, vol. 12, no. 2, pp. 61-93, 1993.
- [33] R. M. M., *Drop-surface interactions*, New York: Springer, 2002.
- [34] C. Stow and M. Hadfield, "An Experimental Investigation of Fluid Flow Resulting from the Impact of a Water Drop with an Unyielding Dry Surface," in *Royal Society A:Mathematical Physical and Engineering Sciences*, 1981.
- [35] C. Mundo, M. Sommerfeld and C. Tropea, "Droplet-wall Collisions: Experimental studies of the deformation and break-up processes," *International Journal of Multiphase Flow*, vol. 21, no. 2, pp. 151-173, 1995.
- [36] K. Perera, B. Sampath, V. Dassanayake and B. Hapuwatte, "Harvesting of Kinetic Energy of the raindrops," *International Journal of Mathematical, Computational, Physical and Quantum Engineering*, vol. 8, no. 2, pp. 325-330, 2014.
- [37] S. Sikalo, M. Marengo, C. Tropea and E. Ganic, "Analysis of impact of droplets on horizontal surfaces," *Experimental Thermal and Fluid Sciences*, vol. 25, pp. 503-510, 2002.
- [38] S. Sikalo, C. Tropea and E. Ganic, "Impact of droplets onto inclined surfaces," *Journal of Colloid and Interface Science*, vol. 286, pp. 661-669, 2005.
- [39] H. Robert, "Stratiform precipitation in Regions of Convection: A meteorological paradox?," *Bulletin of the American Meteorological Society*, vol. 78, no. 10, pp. 2179-2196, 1997.
- [40] P. Biswas, M. Uddin, M. Islam, M. Sarkar, V. Desa, M. Khan and A. Huq, "Harnessing raindrop energy in Bangladesh," in *International Conference on Mechanical Engineering*, Dhaka, 2009.
- [41] F. Viola, P. Romano, R. Miceli and G. Acciari, "Harvesting rainfall energy by means of piezoelectric transducer," in *International conference on Clean Electrical Power*, Alghero, 2013.
- [42] W. Chin-Hong, Z. Dahari, A. Abd Manaf, O. Sidek, M. Miskam and J. Mohamed, "Simulation of piezoelectric raindrop energy harvester," in *TENCON*, Sydney, 2013.
- [43] C.-H. Wong, Z. Dahari, A. A. Manaf and M. A. Miskam, "Harvesting Raindrop Energy with Piezoelectrics: a Review," *Journal of Electronic Materials*, vol. 44, no. 1, pp. 13-21, 2015.
- [44] C. Josserand and S. Zaleski, "Droplet splashing on a thin liquid film," *Physics of Fluids*, vol. 15, no. 6, pp. 1650-1657, 2003.

- [45] Y. C. Shu and I. C. Lien, "Efficiency of energy conversion for a piezoelectric power harvesting system," *Journal of Micromechanics and Microengineering*, vol. 16, pp. 2429-2438, 2006.
- [46] E. K. Reily, F. Burghardt, R. Fain and P. Wright, "Powering a wireless sensor node with a vibration-driven piezoelectric energy harvester," *Smart Materials and Structures*, vol. 20, 2011.
- [47] APS Group Scotland, "Drinking Water Quality in Scotland 2013: Public Water Supply," Drinking Water Quality Regulator for Scotland, 2014.
- [48] B. F. Edwards, J. W. Wilder and E. E. Scime, "Dynamics of falling raindrops," *European Journal of Physics*, vol. 22, pp. 113-118, 2001.
- [49] A. M. MacDonald and B. Dochartaigh, "Baseline Scotland: an overview of available groundwater chemistry data for Scotland," British Geological Survey, 2005.
- [50] World Health Organization, "Nutrients in Drinking Water," WHO Press, Geneva, 2005.
- [51] I. P. Lipscomb, P. M. Weaver, J. Swingler and J. W. McBride, "The effect of relative humidity, temperature and electrical field on leakage currents in piezo-ceramic actuators under dc bias," *Sensors and Actuators A: Physical*, vol. 151, no. 2, pp. 179-186, 2009.
- [52] I. P. Lipscomb, P. M. Weaver, J. Swingler and J. W. McBride, "Micro-computer tomography-An aid in the investigation of structural changes in lead zirconate titanate ceramics after temperature-humidity bias testing," *Journal of Electroceramics*, vol. 23, no. 1, pp. 72-75, 2009.
- [53] N. B. Vargaftik, B. N. Volkov and L. D. Voljak, "International Tables of the Surface Tension of Water," *Journal of Physical and Chemical Reference Data*, vol. 12, no. 3, pp. 817-820, 1993.
- [54] S. Xu, J. Cui and X. Ren, "Applied Mechanics and Engineering Model on Raindrops falling," in *International Conference on Electronic and Mechanical Engineering and Information Technology*, Heilongjiang, 2012.

641

642

Mohammad Adnan Ilyas received a BEng (Hons) in Electrical and Electronic Engineering from Heriot-Watt University, UK in 2012 followed by a MSc in Renewable Energy and Distributed Generation from Heriot-Watt University, UK in 2013. He is currently pursuing a PhD in Electrical Engineering researching on 'Energy Harvesting for a 12V DC System' at Heriot-Watt University, UK.

Jonathan Swingler received a Joint BSc (Hons) in Physics and Chemistry from Keele University, UK, in 1990 followed by a PhD at Loughborough University, UK, for his work into the degradation of electrical contacts. He subsequently moved to the University of Southampton, UK, where he pursued his research into the physics of degradation and reliability of electrical/electronic materials and devices. Currently Jonathan is developing reliability engineering science in connection with energy systems at Heriot-Watt University, UK. His is an Associate Professor of Energy at Heriot-Watt University and Fellow of the Institute of Physics.